

**ICSV14**  
Cairns • Australia  
9-12 July, 2007



## **PERFORMANCE OF PERFORATED FACING ABSORBERS**

Robert Hooker

Division of Mechanical Engineering, The University of Queensland  
Brisbane, QLD 4072, Australia  
[rjhjhadv@powerup.com.au](mailto:rjhjhadv@powerup.com.au)

### **Abstract**

The paper presents extended results from a study of the effect of air-gaps in absorbers with perforated facing. Normal incidence absorption coefficient is measured for a wide range of parameters. There are two facing arrangements, each with open area 14% but with two different hole sizes, 2.5 and 6.35 mm. The cavity behind the facing ranges from 100 to 350 mm in several steps. Absorbent material in the cavity is glasswool in either 50 or 75 mm thickness, placed over the entire range from no gap in front of the absorbent to no gap behind the absorbent. The empty cavity is included. Experimental results are compared with coefficients calculated using a prediction package.

The measurements use the travelling microphone technique in the impedance tube method and approaches that allow an extended frequency range are presented.

### **1. INTRODUCTION**

An initial interest in the development of roadside noise barriers has led to an extended study of the effect of absorbent material and air-gaps for sound absorber treatments with perforated facings. Two facings have been tested, each with an open area of 14%. One facing has 2.5 mm diameter holes in a square pattern of pitch 5.5 mm, the other has 6.35 mm diameter holes in an equilateral triangular pattern of pitch 16.5 mm. The space behind the facing is varied up to 350 mm and absorbent material is placed in this space. The absorbent material is glasswool of density 48 kg/cu m and two thicknesses are used, 50 and 75 mm. The position of the absorbent material is varied in steps from no gap between absorbent and facing to no gap behind the absorbent. The normal incidence absorption coefficient has been determined from measurements in an impedance tube using the travelling microphone method. This paper is an extension of a previous presentation [1].

### **2. THE IMPEDANCE TUBE**

The travelling microphone (with probe) method of measuring the standing wave in an impedance tube was used. This is a slow and tedious technique but the operation of the tube is automated so the tedium is somewhat relieved. The recording system enables the standing

wave pattern to be displayed over the full test length and in every case the pattern was checked to ensure a valid result. This will be shown to be important at the extremes of frequency range.

Typical patterns are shown in Figures 1 to 4. In Figure 1, the points (+) are pressure-squared values calculated from the experimental dB data (+) shown in Figure 2. The nature of the standing wave is that the pressure-squared plot against distance along the tube should be a sinusoid. A sinusoid is fitted to the experimental data of Figure 1 by setting the magnitude and position of the minimum, the value of the maximum, and specifying the frequency. The fitted sinusoid is a line in the figure (visible when the figure is enlarged). A line is added to Figure 2 as the dB plot calculated from the fitted pressure-squared sinusoid (visible near the first minimum). It can be seen that the standing wave is indeed sinusoidal and that the fitted result matches the experimental data in both pressure-squared and decibel plots. Figures 3 and 4 present similar material for a different frequency. The configuration key for the figures is given at the bottom of this page.

The one impedance tube was used for frequencies from 125 to 4000 Hz. This is a greater frequency range than is normally accepted [2,3] for one tube. The tube has a square cross-section, internal dimension 82.5 mm. The corresponding upper frequency limit (ISO 10534-1) is 2080 Hz. Above this frequency transverse waves might occur and the longitudinal waves might not be plane. When testing at 4000 Hz, the frequency was changed slightly to produce a longitudinal resonance in the tube. Also, the probe in the tube is terminated by a four-prong end, with the probe openings on the quarter points of the tube diagonals. This arrangement cancels the first three transverse wave effects. It has been confirmed for this tube by transverse traverses that plane wave conditions will normally be achieved at longitudinal resonances. Also, by viewing every recorded pattern it can be verified that a true standing wave is present. Occasionally a true pattern is not achieved and in that case the result is discarded. Figures 5 and 6 show a typical result near 4000 Hz, the frequency having been set at 3880 Hz as a longitudinal resonance.

The tube length is 0.9 m and ISO 10534-1 specifies a lower frequency limit of 380 Hz in order to ensure two pressure minima are observed. The requirement for two minima is set in order to extrapolate the minima back to the test specimen face to correct for energy absorption by the walls of the tube. This tube has steel walls 3.2 mm thick and the observed pressure minima are typically equal and rarely differ by as much as 0.2 dB (see, for example, Figures 2 and 4). Even this difference will affect absorption coefficient by 0.02 or less. The tube length condition can be relaxed to allow one minimum and one maximum. Further, if one minimum is well defined and a suitable length of trace is available, it is possible to fit a sinusoid to the pressure-squared trace and hence predict the maximum. Figures 7 and 8 give a result for a frequency of 125 Hz. To fit the part-sinusoid, the magnitude and position values are set at the observed minimum, the frequency is set and the maximum determined by trial and error to achieve best fit. A change of 0.1 dB in the maximum value produces a noticeable change in the fitted trace and it is easily possible to set the maximum to 0.1 dB by eye. Thus the procedures outlined enable the range extensions adopted.

The configuration codes used in the figures and tables are as follows: -

Perforated facing: S = small holes; L = large holes.

Air-gap: In mm.

Absorbent: A50 = 50 mm thick; A75 = 75 mm thick.

Air-gap: In mm.

Thus the code S-50-A50-100 indicates facing with small holes, 50 mm air-gap, 50 mm glasswool, 100 mm air-gap, total cavity 200 mm. In all cases the tube was closed by a solid steel end.

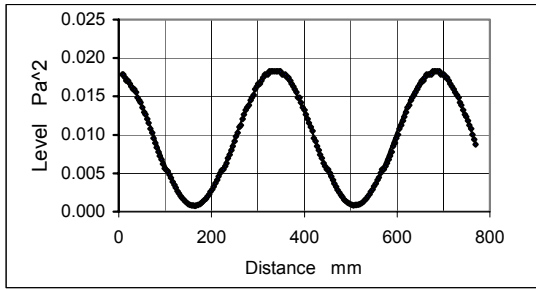


Figure 1. Pressure-squared. 500 Hz. S-0-A50-250.

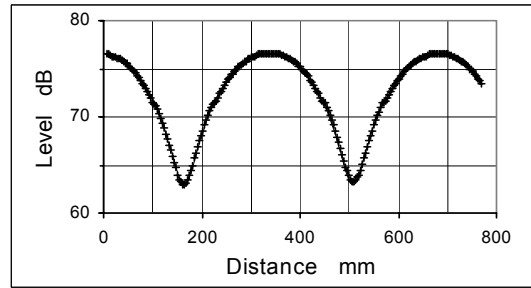


Figure 2. Decibel plot. 500 Hz. S-0-A50-250.

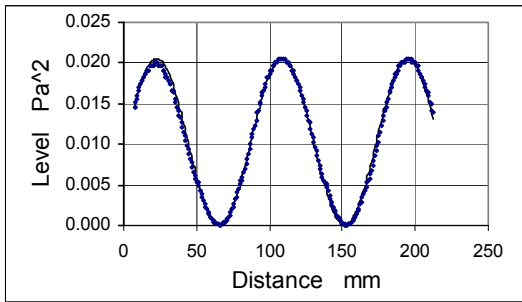


Figure 3. Pressure-squared. 2000 Hz. L-200

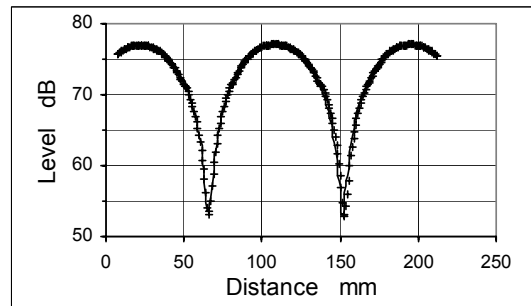


Figure 4. Decibel plot. 2000 Hz. L-200.

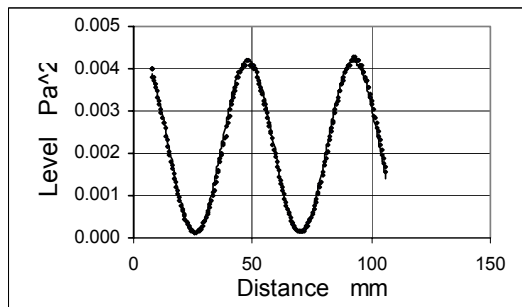


Figure 5. Pressure-squared. 3880 Hz. S-25-A50-25.

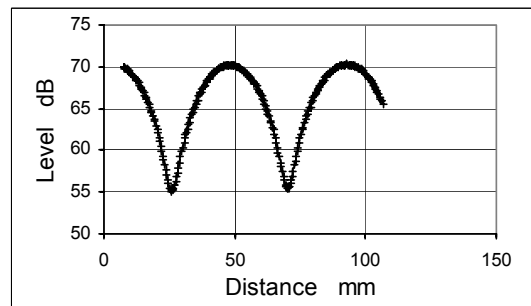


Figure 6. Decibel plot. 3880 Hz. S-25-A50-25.

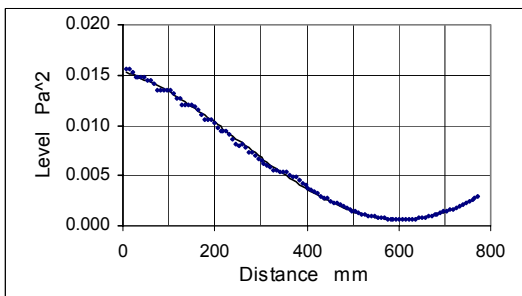


Figure 7. Pressure-squared. 125 Hz. S-100

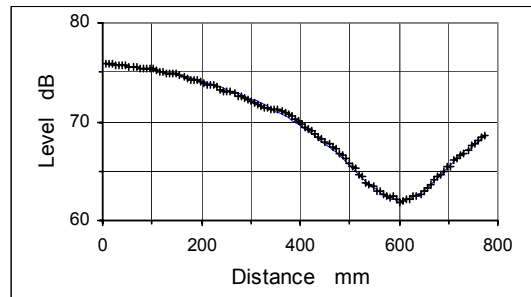


Figure 8. Decibel plot. 125 Hz. S-100.

Absorption coefficients:

Figures 1 & 2: 0.57

Figures 3 & 4: 0.22

Figures 5 & 6: 0.51

Figures 7 & 8: 0.55

### 3. EXPERIMENTAL RESULTS

Tests were conducted over a wide range of conditions. Background checks included a reflecting end, the absorbent material alone and the perforated facings with air-gap and no absorbent. Results for cavities 200 and 300 mm with all combinations of hole sizes and absorbent thickness are given in Tables 1 and 2. Results for other cavities are given in Tables 4 and A2.

Table 1. Absorption coefficients. Cavity 200 mm.

Configuration	Frequency Hz					
	125	250	500	1000	2000	4000
S-200	0.29	0.20	0.17	0.11	0.52	0.16
L-200	0.27	0.24	0.19	0.24	0.22	0.05
S-0-A50-150	0.67	0.78	0.71	0.91	0.91	0.72
S-25-A50-125	0.70	0.79	0.80	0.89	0.79	0.47
S-50-A50-100	0.64	0.81	0.86	0.83	0.62	0.71
S-75-A50-75	0.53	0.76	0.92	0.70	0.86	0.61
S-100-A50-50	0.47	0.67	0.92	0.76	0.91	0.66
S-125-A50-25	0.37	0.58	0.90	0.71	0.66	0.59
S-150-A50-0	0.29	0.43	0.64	0.87	0.69	0.50
S-0-A75-125	0.64	0.68	0.68	0.89	0.92	0.73
S-25-A75-100	0.63	0.80	0.80	0.98	0.85	0.46
S-50-A75-75	0.58	0.81	0.85	0.90	0.62	0.71
S-75-A75-50	0.53	0.79	0.88	0.78	0.76	0.45
S-100-A75-25	0.44	0.73	0.90	0.70	0.92	0.55
S-125-A75-0	0.38	0.63	0.89	0.70	0.71	0.50
L-0-A50-150	0.68	0.93	0.76	0.96	0.79	0.64
L-50-A50-100	0.57	0.98	0.94	0.86	0.52	0.58
L-100-A50-50	0.46	0.85	0.95	0.68	0.79	0.56
L-150-A50-0	0.40	0.48	0.73	0.83	0.52	0.48
L-0-A75-125	0.72	0.85	0.77	0.92	0.78	0.43
L-25-A75-100	0.69	0.94	0.88	0.98	0.66	0.28
L-50-A75-75	0.65	0.94	0.93	0.87	0.51	0.40
L-100-A75-25	0.47	0.82	0.93	0.68	0.77	0.36
L-125-A75-0	0.36	0.64	0.88	0.70	0.54	0.31

Results can be plotted with either gap or frequency as parameter (see figures in the Appendix). However, the author's experience in this and other projects is that with only a little experience it is possible to run one's eye along chosen rows or columns in the tables and picture the trends and relative performances. This is easier than making multiple graphs and unravelling their intertwining lines.

The highest absorption is generally in the 500 to 2000 Hz range and there are some surprisingly small coefficients at 4000 Hz. The mid-frequency range has been examined by calculating the average of the 250, 500, 1000 and 2000 Hz coefficients, i.e., the noise reduction coefficient (NRC). The highest is 0.89 for configuration S-25-F50-25) and the second is 0.87 for S-175-F75-50. The latter result is out of character since in every other case the highest NRC is with zero or small gap in front. The case of zero gap behind always has the smallest NRC. Excluding those cases, NRC ranges from 0.71 to 0.87.

Table 2. Absorption coefficients. Cavity 300 mm.

Configuration	Frequency Hz					
	125	250	500	1000	2000	4000
S-300	0.25	0.27	0.13	0.10	0.26	0.10
L-300	0.32	0.22	0.15	0.08	0.18	0.11
S-0-A50-250	0.79	0.80	0.57	0.83	0.92	0.64
S-50-A50-200	0.77	0.88	0.77	0.90	0.62	0.54
S-100-A50-150	0.70	0.86	0.84	0.64	0.90	0.43
S-150-A50-100	0.58	0.83	0.84	0.73	0.69	0.40
S-200-A50-50	0.40	0.66	0.81	0.94	0.76	0.42
S-250-A50-0	0.23	0.35	0.62	0.81	0.86	0.45
S-0-A75-225	0.66	0.66	0.62	0.84	0.91	0.72
S-25-A75-200	0.70	0.80	0.75	0.96	0.82	0.45
S-50-A75-175	0.70	0.82	0.78	0.93	0.63	0.71
S-75-A75-150	0.68	0.84	0.80	0.83	0.75	0.46
S-125-A75-100	0.63	0.86	0.82	0.71	0.68	0.56
S-175-A75-50	0.50	0.82	0.80	0.90	0.95	0.63
S-225-A75-0	0.36	0.60	0.79	0.91	0.62	0.69
L-0-A50-250	0.80	0.88	0.66	0.86	0.79	0.60
L-50-A50-200	0.77	0.94	0.88	0.92	0.55	0.58
L-100-A50-150	0.66	0.99	0.92	0.68	0.80	0.53
L-150-A50-100	0.52	0.98	0.83	0.72	0.54	0.48
L-200-A50-50	0.47	0.76	0.79	1.00	0.65	0.45
L-250-A50-0	0.34	0.46	0.69	0.81	0.62	0.45
L-0-A75-225	0.74	0.71	0.71	0.87	0.82	0.48
L-25-A75-200	0.74	0.80	0.80	0.99	0.59	0.29
L-50-A75-175	0.75	0.87	0.85	0.88	0.47	0.44
L-75-A75-150	0.73	0.89	0.85	0.74	0.68	0.31
L-125-A75-100	0.66	0.94	0.80	0.63	0.50	0.38
L-175-A75-50	0.55	0.87	0.74	0.94	0.86	0.44
L-225-A75-0	0.40	0.58	0.73	0.84	0.48	0.43

For all cavities except 100 mm, the average NRC for each group (same hole size and absorbent thickness) lies in the range 0.77 to 0.80. The range for 100 mm cavity is 0.79 to 0.84, i.e., a cavity of 100 mm is as good as any.

The results in Tables 1 and 2 are given for particular cavities with the absorbent layer shifted progressively from the front to the back. An alternative presentation is for a particular air-gap on one side of the absorbent layer and a progressively changing gap on the other side. A selection of results in that format is shown in the Appendix, Table A1, where the gap between facing and absorbent is constant in each group, and in Figure A1 (upper) with the gap behind the absorbent kept constant.

#### 4. CALCULATED RESULTS AND COMPARISONS

A method for calculating the absorption coefficient of multi-layer arrangements is available from Ingard [4]. Program 141 is a procedure to calculate normal incidence and diffuse field coefficients and can be applied to combinations of perforated plates, air-gaps and porous layers. A normalised flow resistance parameter R must be specified to characterise the porous layer. The absorption coefficients of the glasswool material were measured and trial values of R that best fitted these results were selected. The calculated and experimental results agree in

general form but differ at 125 and 500 Hz, see Table 3. Experimental and calculated results for cavity 100 mm are given in Table 4.

Table 3. Representation of glasswool material.

Test	Frequency Hz					
	125	250	500	1000	2000	4000
A50, expt.	0.32	0.32	0.72	0.88	0.91	0.97
A50, calc,R=1.7	0.10	0.32	0.66	0.89	0.93	0.98
A75, expt.	0.48	0.52	0.85	0.85	0.92	0.97
A75, calc,R=1.7	0.27	0.55	0.76	0.85	0.93	0.98

Table 4. Cavity 100 mm.

Configuration	Frequency Hz					
	125	250	500	1000	2000	4000
<b>Experiment</b>						
S-0-A50-50	0.55	0.69	0.86	0.90	0.92	0.65
S-25-A50-25	0.53	0.69	0.95	0.97	0.93	0.51
S-50-A50-0	0.49	0.49	0.91	0.97	0.73	0.56
S-0-A75-25	0.56	0.69	0.87	0.91	0.92	0.64
S-25-A75-0	0.46	0.46	0.93	0.99	0.75	0.52
L-0-A50-50	0.56	0.69	0.85	0.86	0.79	0.46
L-25-A50-25	0.55	0.69	0.97	0.99	0.76	0.35
L-50-A50-0	0.46	0.54	0.95	0.94	0.53	0.39
L-0-A75-25	0.46	0.66	0.86	0.90	0.78	0.43
L-25-A75-0	0.42	0.54	0.98	0.97	0.59	0.38
<b>Calculation</b>						
S-0-A50-50	0.35	0.66	0.84	0.93	0.84	0.41
S-25-A50-25	0.23	0.56	0.88	0.98	0.54	0.30
S-50-A50-0	0.11	0.37	0.79	0.79	0.50	0.31
S-0-A75-25	0.39	0.65	0.81	0.95	0.86	0.41
S-25-A75-0	0.28	0.60	0.87	0.97	0.55	0.31
L-0-A50-50	0.36	0.68	0.88	0.94	0.54	0.18
L-25-A50-25	0.24	0.60	0.95	0.87	0.28	0.14
L-50-A50-0	0.11	0.40	0.83	0.60	0.29	0.13
L-0-A75-25	0.40	0.67	0.85	0.96	0.57	0.18
L-25-A75-0	0.28	0.64	0.94	0.87	0.30	0.14

The 100 mm cavity results show that good absorption coefficients can be achieved without a need for deeper cavities. The agreement between experimental and calculated results is good in parts. The trends are similar and results generally agree from 250 to 2000 Hz but agreement is not good at the extremes of frequency. An advantage of the calculation procedure is that it will also give the diffuse incidence coefficient. Hence, where there is reasonable agreement between calculation and experiment for normal incidence it seems reasonable to use the calculation to predict diffuse field behaviour, at least to select configurations for diffuse field testing.

## 5. CONCLUSION

The purpose of this study was to assess the relative performance of different hole sizes in the perforated facing (for the same percentage open area), of different placing and thickness of absorbent and of different cavity sizes. There are a few isolated cases of high absorption coefficients but in general the different hole sizes and absorbent placing and thickness had no appreciable effect (except for the poor performance with zero gap behind the absorbent).

The major outcome from the study is that the performance of the 100 mm cavity is as good as or better than that of the larger cavities in the mid-frequencies. Unless particular peaks from the coefficient tables are to be utilised there is no point in a larger cavity for 250 Hz and above. The 100 mm cavity is inferior at 125 Hz. Greater absorbent thickness could be used in the larger cavities so the question arises of whether higher coefficients would then be obtained. The reasonable agreement noted between experimental and calculated results (Ingard 141) suggests that a calculation approach is appropriate for an initial investigation of the effect of greater absorbent thickness.

A further useful feature of the calculation procedure is that it allows extension to the diffuse field case.

## REFERENCES

- [1] R.J. Hooker, "The effect of air-gaps in absorbers with perforated facing", *Internoise 2004*, Prague, Czech Republic, 22-25 August 2004, Paper 826.
- [2] ISO10534-1:1996 Acoustics - Determination of sound absorption coefficient in impedance tubes Part 1: Method using standing wave ratio.
- [3] ASTM C384-901 Standard test method for impedance and absorption of acoustical materials by the impedance tube method. Amer. Soc. Testing and Matls., 04-06, 1990, 100-110.
- [4] K. Ingard, *Notes on sound absorption technology*, Noise Control Foundation, 1994.

## APPENDIX

Table A1. Absorption coefficients. In "gap-in-front" groups.

Configuration	Frequency Hz					
	125	250	500	1000	2000	4000
S-25-A50-25	0.53	0.69	0.95	0.97	0.93	0.51
-125	0.70	0.79	0.80	0.89	0.79	0.47
S-50-A50-0	0.49	0.49	0.91	0.97	0.73	0.56
-100	0.64	0.81	0.86	0.83	0.62	0.71
-200	0.77	0.88	0.77	0.90	0.62	0.54
S-25-A75-0	0.46	0.46	0.93	0.99	0.75	0.52
-100	0.63	0.80	0.80	0.98	0.85	0.46
-200	0.70	0.80	0.75	0.96	0.82	0.45
S-50-A75-75	0.58	0.81	0.85	0.90	0.62	0.71
-175	0.70	0.82	0.78	0.93	0.63	0.71
L-25-A50-25	0.55	0.69	0.97	0.99	0.76	0.35
L-50-A50-0	0.56	0.69	0.85	0.86	0.79	0.46
-100	0.57	0.98	0.94	0.86	0.52	0.58
-150	0.67	0.96	0.91	0.83	0.56	0.57
-200	0.77	0.94	0.88	0.92	0.55	0.58
-250	0.86	0.93	0.81	0.84	0.53	0.46
L-25-A75-0	0.42	0.66	0.86	0.90	0.78	0.43
-100	0.69	0.94	0.88	0.98	0.66	0.28
-200	0.74	0.80	0.80	0.99	0.59	0.29
L-50-A75-75	0.65	0.94	0.93	0.87	0.51	0.40
-175	0.75	0.87	0.85	0.88	0.47	0.44
-225	0.73	0.79	0.80	0.84	0.46	0.52

Table A2. Absorption coefficients. Cavities 250 and 350 mm.

Configuration	Frequency Hz					
	125	250	500	1000	2000	4000
Cavity 250 mm						
L-0-A50-200	0.77	0.88	0.72	0.87	0.83	0.60
L-50-A50-150	0.67	0.96	0.91	0.83	0.56	0.57
L-100-A50-100	0.56	0.98	0.94	0.61	0.82	0.52
L-150-A50-50	0.49	0.84	0.85	0.73	0.57	0.45
L-200-A50-0	0.36	0.46	0.67	0.98	0.70	0.42
Cavity 350 mm						
L-0-A50-300	0.83	0.90	0.57	0.92	0.81	0.52
L-50-A50-250	0.86	0.93	0.81	0.84	0.53	0.46
L-100-A50-200	0.72	0.97	0.86	0.68	0.76	0.40
L-150-A50-150	0.53	0.99	0.76	0.88	0.57	0.37
L-200-A50-100	0.56	0.94	0.74	0.96	0.61	0.38
L-250-A50-50	0.49	0.80	0.77	0.73	0.73	0.32
L-300-A50-0	0.34	0.41	0.80	0.77	0.53	0.34
L-0-A75-275	0.64	0.67	0.69	0.88	0.81	0.57
L-50-A75-225	0.73	0.79	0.80	0.84	0.46	0.52
L-150-A75-125	0.65	0.83	0.67	0.79	0.55	0.41
L-250-A75-25	0.48	0.55	0.70	0.65	0.75	0.55
L-275-A75-0	0.45	0.45	0.74	0.60	0.70	0.43

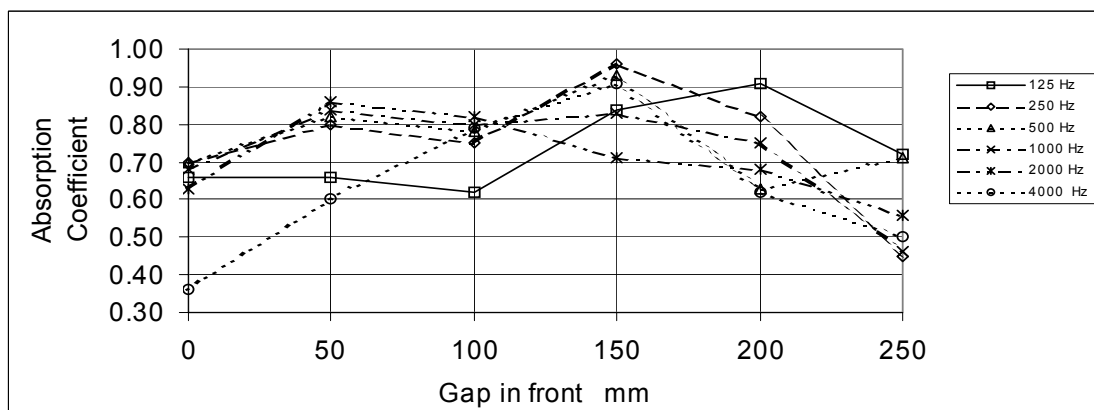
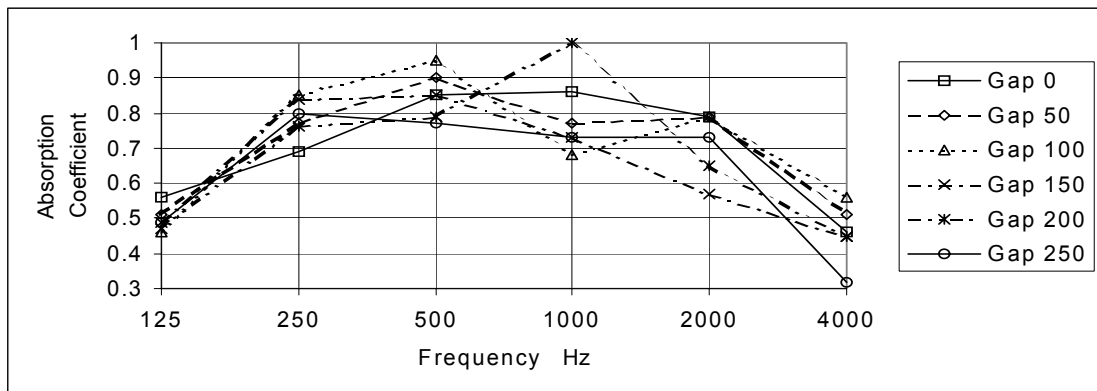


Figure A1. Upper, L-x-A50-50. Lower, L-x-A50-y, cavity 300 mm.